

# The metallicity of the high column density $\text{Ly}\alpha$ forest at $2 < z < 3.5$

Tae-Sun Kim<sup>1</sup>

<sup>1</sup>Institute of Astronomy, Madingley Road, Cambridge CB3 0HA, UK  
email: tkim@ast.cam.ac.uk

**Abstract.** We have studied the metallicity of 17 high column density forests at  $N_{\text{H I}} = 10^{15-17} \text{ cm}^{-2}$  and  $2 < z < 3.5$  toward 7 high- $z$  QSOs taken with the VLT/UVES, in order to study the metallicity of absorption line systems as a function of H I column density and  $z$ . This relation provides an important constraint on metal enrichment mechanisms of the intergalactic medium as well as early star formation in galaxies. We used higher order Lyman series to measure a reliable H I column density for the saturated  $\text{Ly}\alpha$  lines, and applied an ionisation correction assuming the Haardt-Madau UV background including both galaxies and QSOs. We have found 3, 6, and 8 systems with no metals, C IV-only, and additional ions other than C IV respectively. A photoionisation model with the Haardt-Madau background generally reproduces the observed metal line ratios. The median [C/H] is  $-3.03$  and  $-1.96$  for the 6 C IV-only systems and the 8 additional-ion systems respectively. The inferred H I number density is  $n_{\text{H I}} \sim 10^{-3.5} \text{ cm}^{-3}$  and  $\sim 10^{-2.5} \text{ cm}^{-3}$  for the C IV-only systems and the additional-ion systems respectively. When other ions are present, [C/H] of the high- $N_{\text{H I}}$  forest is similar to that of sub-damped  $\text{Ly}\alpha$  systems.

## 1. Introduction

In the paradigm of current hydrodynamic simulations, the low column density neutral hydrogen (H I) QSO absorption systems, the  $\text{Ly}\alpha$  forest, arise from the diffuse intergalactic medium (IGM) of filamentary and sheet-like structures, while higher column density QSO absorption line systems such as Lyman limit systems and damped  $\text{Ly}\alpha$  systems (DLA) are believed to be produced by intervening galaxies or halos connecting the IGM filaments and sheets where galaxies form. In short, the higher the column density an absorption system is, the more likely it is that the system is close to one of these halo structures, and the more easily the system is enriched by nearby star-forming galaxies (Aguirre *et al.* 2001).

Therefore, metals in the IGM, mainly probed by the  $\text{Ly}\alpha$  forest, contain an important record of past star formation activity and of the feedback of galactic matter into the IGM, because metals are produced only by stars which are bound in galaxies (Schaye *et al.* 2003). While the nature in which metals are transported out of galaxies is not well established, different trends between the metallicity and the column density of absorption systems are expected, depending on different mechanisms. If we take a supernovae-driven super-wind to be the main mechanism, and if this mechanism is very effective, we would expect a monotonic correlation between the metallicity and the absorption column density. Therefore, the metallicity as a function of  $N_{\text{H I}}$  as well as  $z$  would provide a valuable constraint on the enrichment mechanism.

Early studies have shown that  $\sim 90\%$  of the forest systems with H I column density greater than  $N_{\text{H I}} > 10^{15} \text{ cm}^{-2}$  are enriched with C IV (Songaila & Cowie 1996) and even with O VI (Carswell *et al.* 2002) at  $z \sim 2-3$ . Schaye *et al.* (2003) find that [C/H] in the IGM is highly inhomogeneous, and over-density-dependent but  $z$ -independent: [C/H]

$\sim -3.5$ ,  $2 < z < 4.5$ . On the other hand, DLAs and sub-DLAs ( $N_{\text{HI}} > 10^{19} \text{ cm}^{-2}$ ) having a wider range of metals than carbon and oxygen show higher metal abundances,  $[\text{M}/\text{H}] \sim -1.5$  with a large scatter, and they are weakly  $z$ -dependent in the range  $1.5 < z < 4.5$  (Prochaska *et al.* 2003).

Unfortunately, studies of the metallicity of absorption systems at  $N_{\text{HI}} = 10^{15-19} \text{ cm}^{-2}$  have been largely neglected due to the three main difficulties: 1) their HI Ly $\alpha$  lines are heavily saturated, thus  $N_{\text{HI}}$  cannot be measured reliably; 2) The ionisation correction is large and very uncertain due to the unreliable  $N_{\text{HI}}$  values; and 3) in case of the Lyman limit systems at  $N_{\text{HI}} = 10^{17.2-19} \text{ cm}^{-2}$  the metallicity is sensitive to the assumed UV background. Unlike the optically thin forest, the optically thick Lyman limit systems are likely to be closer to galaxies and require a UV background contribution from both the meta-galactic UV background and the unknown local ionising sources. Therefore, it is limited by an even more unreliable ionisation correction.

In our first step to studying the metallicity as a function of  $N_{\text{HI}}$  and  $z$  at  $N_{\text{HI}} = 10^{15-19} \text{ cm}^{-2}$  in the range  $2 < z < 3.5$ , we concentrate on the high column density forest at  $N_{\text{HI}} = 10^{15-17} \text{ cm}^{-2}$ , because they are simpler to interpret than the Lyman limit systems. Here, we present our study on the metallicity of 17 high column density forests toward 7 high- $z$  QSOs obtained using the UVES at the VLT. Due to its blue sensitivity, all of the 7 QSOs were observed from  $\sim 10,000 \text{ \AA}$  down to the atmospheric cutoff,  $\sim 3050 \text{ \AA}$ . This wavelength coverage enables us to use the higher order Lyman series other than Ly $\alpha$  to measure a reliable  $N_{\text{HI}}$ . Since the most abundant ion in the forest is C IV, we use the abundance of carbon as an indicator of the metallicity of the forest. In Section 2, observations and data reduction are discussed. The results are in section 3 and the conclusions are in section 4.

## 2. Observations and data reduction

Table 1 lists the QSOs analysed in this study. The data were taken from the ESO archive and were observed with the VLT/UVES. The spectra were reduced with the MIDAS/UVES package and the resolution was about  $R \sim 45,000$ . The S/N varies across the spectrum and the typical S/N in the Ly $\alpha$  forest is  $\sim 40-50$  for all the QSOs. The spectra were normalised locally with 5th and 7th-order polynomial fitting. In order to avoid the proximity effect, we only include the Ly $\alpha$  forest  $4,000 \text{ km s}^{-1}$  short-ward of the Ly $\alpha$  emission.

We adopted our analysis based on the Voigt profile fitting using VPFIT (Carswell *et al.* 2001). Firstly, metal lines were identified in the individual spectrum. Secondly, the rest of the absorption lines were fitted including the already fitted metal lines. The high- $N_{\text{HI}}$  forest which is our main interest was saturated. For the saturated lines, the derived  $N_{\text{HI}}$  is only a *lower* limit if measured using only Ly $\alpha$ . Due to their lower oscillator strength, the higher orders of the Lyman series are often found not to be saturated, as long as they are not blended with lower- $z$  forest. Therefore, we used the entire spectrum down to  $3050 \text{ \AA}$ , fitting the Ly $\alpha$  lines with the higher orders of Lyman series and adding the lower- $z$  Ly $\alpha$  lines simultaneously. During this process, the continuum was re-adjusted by small amounts to obtain a satisfactory fit for all Lyman series including all the identified metal lines.

We only analysed the high- $N_{\text{HI}}$  forest when it was fitted at least with Ly $\beta$ , which restricts the redshift ranges in our sample to be  $z > 1.986$ . Since the forest at  $z < 2.14$  did not cover the Lyman series higher than Ly $\gamma$  (due to the observed wavelength cutoff below  $3050 \text{ \AA}$ ), the reliability of the measured  $N_{\text{HI}}$  at  $z < 2.14$  is not as good as that at  $z > 2.14$ . Note that there is in general a trade-off between the availability of higher order

**Table 1.** The QSOs analysed

QSOs	$z_{\text{em}}$	Forest redshifts	Number of analysed systems
PKS1448–232	2.219	1.986–2.175	1
PKS0237–23	2.223	1.986–2.179	1
HE2217–2818	2.406	1.986–2.360	3
HE1122–1648	2.412	1.986–2.365	2
Q0329–385	2.435	1.986–2.389	2
Q0002–422	2.767	2.183–2.717	6
PKS2126–158	3.280	2.669–3.222	5

Lyman series and  $z$ . At higher  $z$ , the high- $N_{\text{HI}}$  forest usually covers from Ly $\alpha$  to Ly $\kappa$ , if not down to the Lyman limit, but line blending becomes so severe that it sometimes becomes difficult to derive a reliable  $N_{\text{HI}}$ . At lower  $z$ , the high- $N_{\text{HI}}$  forest only extends down to Ly $\gamma$ , but the line blending is much less severe so that the derived  $N_{\text{HI}}$  can be more reliable than the one at higher  $z$ . The significance of each effect, however, depends on the individual system. Table 1 lists the number of high- $N_{\text{HI}}$  forest systems analysed in this study.

### 3. Results

#### 3.1. Observational results

Among the 17 systems in this study, we classified the forest into 3 groups depending on the metals associated with the forest: with no associated C IV over  $3\sigma$ , with C IV only (*the C IV-only systems* throughout this paper) and with additional ions other than C IV (*the additional-ion systems* throughout this paper). There are three systems with no detectable C IV within limits, while there are 6 C IV and 8 additional-ion systems. The additional-ion systems mostly show Si II, Si IV, or O VI. None of the additional-ion systems show Mg II in our sample, clearly showing that our sample does not include any weak Mg II systems. Fig. 1 shows examples of a typical C IV-only and additional-ion systems.

Fig. 2 shows the observed  $N_{\text{C IV}}/N_{\text{HI}}$  as a function of  $N_{\text{HI}}$ . The open squares and open circles are for the additional-ion systems and the C IV-only systems. The open circles with downward arrows indicate the upper limit for the three systems without any detectable metal lines. The stars and open diamonds are taken from Songaila & Cowie (1996) for the partial Lyman limit systems and for the forest respectively at  $z \sim 3$ . Note that their paper does not list an abundance of any other ions so that their sample consists of both the C IV-only and the additional-ion systems. The dot-dashed line indicates the  $3\sigma$  detection limit. Considering most systems in our sample are  $z \sim 2.5$ , there is no strong  $z$ -dependence in  $N_{\text{C IV}}/N_{\text{HI}}$ , despite the small number statistics.

#### 3.2. Photoionisation models

The Ly $\alpha$  forest is highly photoionised. Therefore, an ionisation correction needs to be applied to derive a metallicity. We assume that the forest is in photoionisation equilibrium with the meta-galactic ionising UV background, which is a valid assumption since it is optically thin (Schaye 2001). For the ionisation correction, we use the CLOUDY package (version 94.00, Ferland 2005), under the three assumptions: 1) a plane-parallel geometry, 2) the Solar-abundance pattern, and 3) the Haardt-Madau UV background including contributions from both galaxies and QSOs (Haardt & Madau 2001).

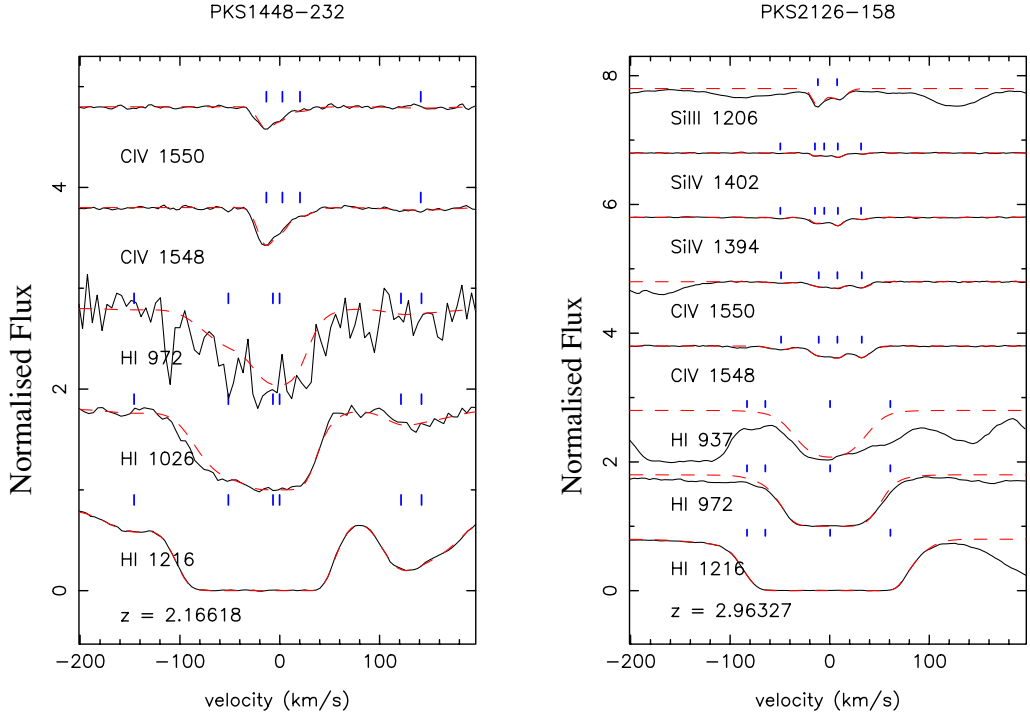


**Figure 1.** Two examples of a typical high- $N_{\text{HI}}$  forest with only C IV (left panel:  $N_{\text{HI}} = 10^{15.1} \text{ cm}^{-2}$ ) and with additional ions (right panel:  $N_{\text{HI}} = 10^{15.8} \text{ cm}^{-2}$ ). The thick dashed lines indicate the fitted profiles, while the thin black lines the data. The thick tick marks indicate the positions of fitted components in velocity space. The origin of the velocity axis is fixed at the strongest H I component.

With two fixed parameters for CLOUDY, the UV background and the observed  $N_{\text{HI}}$ , the two parameters varied were the H I number density  $n_{\text{HI}}$ , and the metal abundance. Since there are always at least two ions present for each system except the 3 metal-free systems, a satisfactory fit to the photoionisation model was always possible. For the C IV-only systems, we used a density estimate based on the  $N_{\text{HI}}$  using a prescription from Schaye (2001), Eq. 8. For the additional-ion systems, both heavy-element abundances and H I number density were varied until the best fit to the observed ion column densities were achieved using the command OPTIMIZE.

The left panel of Fig. 3 shows the derived  $[\text{C}/\text{H}]$  as a function of  $N_{\text{HI}}$ . The open squares and open circles indicate the additional-ion systems and the C IV-only systems, respectively. The filled square indicates one system for which the photoionisation model fails. This system at  $z = 2.251$  toward Q0329–38 clearly shows the velocity difference between C IV (and Si IV) and O VI, which indicates C IV (and Si IV) and O VI do not come from the same region. The stars are the re-calculated  $[\text{C}/\text{H}]$  using the Haardt-Madau UV background from the observational data of Songaila & Cowie (1996), while the open diamonds show  $[\text{C}/\text{H}]$  for the sub-DLAs (Dessauges-Zavadsky *et al.* 2003). The median  $[\text{C}/\text{H}]$  are  $-3.03$  and  $-1.96$  for the 6 C IV-only systems and for the 8 additional-ion systems,

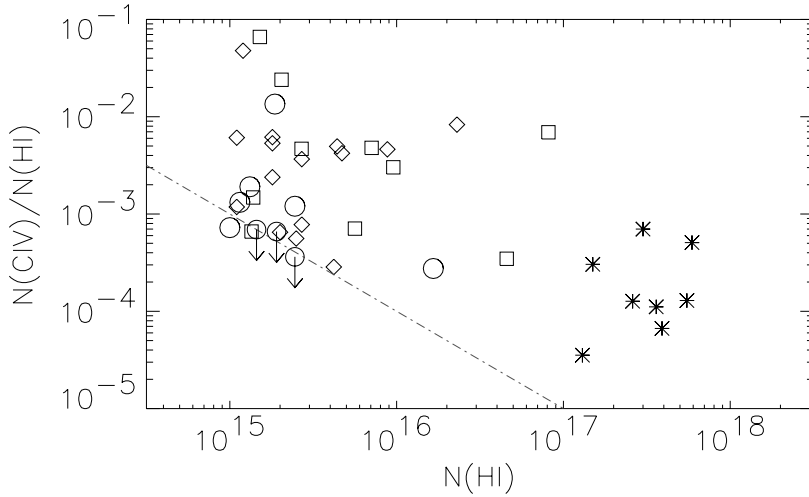


**Figure 2.** The observed  $N_{CIV}/N_{HI}$  as a function of  $N_{HI}$ . The open squares and circles denote the additional-ion systems and the C IV-only systems. The open circles with downward arrows indicate the upper limits. The stars and open diamonds are taken from Songaila & Cowie (1996) for the partial Lyman limit systems and for the forest at  $z \sim 3$  respectively. The dot-dashed line indicates a  $3\sigma$  detection limit.

respectively. The derived  $[C/H]$  values for the 8 additional-ion systems are similar to those of the sub-DLAs. The H I number density is  $10^{-3.5} \text{ cm}^{-3}$  for the 6 C IV-only systems, while it is a factor of 10 higher for the additional-ion systems. The right panel of Fig. 3 shows the derived  $[C/H]$  as a function of  $z$ . There is no strong  $z$ -dependence.

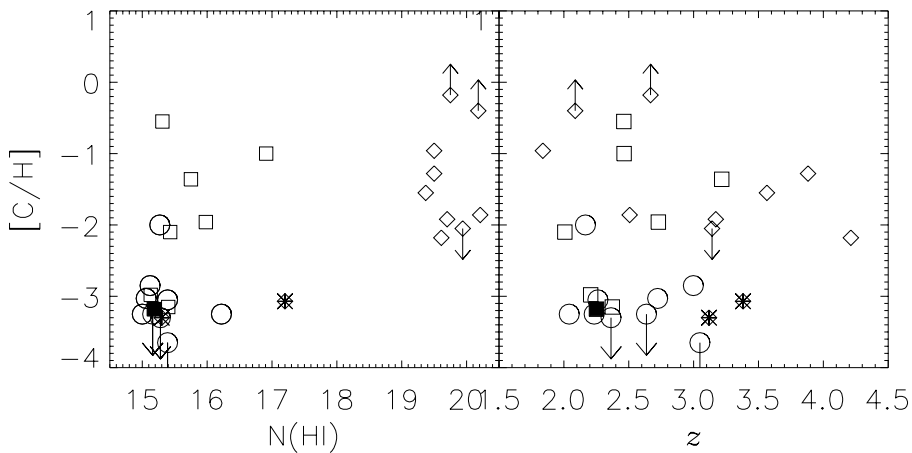


**Figure 3.** Left panel: The derived  $[C/H]$  as a function of  $N_{HI}$ . The diamonds denote the sub-DLAs (Dessauges-Zavadsky *et al.* 2003). The stars show the re-calculated  $[C/H]$  under the assumption of the Haardt-Madau UV background from the observed values of Songaila & Cowie (1996), which is in general a factor of 10 lower than the original  $[C/H]$  in their paper due to the difference in the assumed UV background. Right panel: The derived  $[C/H]$  as a function of  $z$ . The symbols are the same as in the left panel.

## 4. Conclusions

We have studied the  $[C/H]$  abundances of 17 high column density forest systems with  $N_{\text{HI}} = 10^{15-17} \text{ cm}^{-2}$  at  $2 < z < 3.5$  toward 7 high- $z$  QSOs taken with the VLT/UVES. Our aim was to derive the metallicity and HI column density relation for the high- $N_{\text{HI}}$  forest in order to constrain the metal enrichment mechanism. We have fitted the entire available spectrum down to 3050 Å with Voigt profiles and with the high-order Lyman series simultaneously, in order to derive a reliable  $N_{\text{HI}}$  for the saturated high- $N_{\text{HI}}$  forest. In our sample, there are 3 systems without any associated metal lines, 6 systems with only C IV, and 8 systems with additional ions. We assume that the forest is in photoionisation equilibrium with the Haardt-Madau ionising UV background from both galaxies and QSOs. When applied with the ionisation correction using CLOUDY, we have found for the 14 high- $N_{\text{HI}}$  forest:

1. A photoionisation model with the Haardt-Madau background generally reproduces the metal line ratios observed.
2. For the 6 C IV-only systems, the median  $[C/H]$  is  $-3.03$ , the HI number density is  $n_{\text{HI}} \sim 10^{-3.5} \text{ cm}^{-3}$ , and the temperature is  $T \sim 4 \times 10^4 \text{ K}$ .
3. For the 8 systems with additional ions, the inferred  $[C/H]$  is similar to that of sub-DLAs. The median  $[C/H]$  is  $-1.96$ ,  $n_{\text{HI}} \sim 10^{-2.5} \text{ cm}^{-3}$ , and  $T \sim 4 \times 10^4 \text{ K}$ . Despite the small sample size,  $[C/H]$  in the high- $N_{\text{HI}}$  forest increases by a factor of 10 when additional-ions are present compared to the systems with only C IV.
4. Assuming an over-density of  $\sim 70$  for the high- $N_{\text{HI}}$  forest, the measured  $[C/H]$  is consistent with the  $[C/H]$  obtained using the pixel optical depth method of Schaye *et al.* (2003).

## Acknowledgements

I am grateful to the ESO archive for this study. Without it, the work would not have been possible. I also owe R. F. Carswell a debt of gratitude for the photoionisation modelling used in this study.

## References

- Aguirre, A., Hernquist, L., Schaye, J., Katz, N., Weinberg, D. H., Gardner, J., 2001, ApJ, 561, 52
- Carswell, R. F., Schaye, J., Kim, T.-S., 2003, MNRAS, 578, 43
- Carswell, R. F., Webb, J. K., Cooke, A. J., Irwin, M. J., 2001, <http://www.ast.cam.ac.uk/~rfc/vpfit.html>
- Dessauges-Zavadsky, M., Péroux, C., Kim, T.-S., D'Odorico, S., McMahon, R. G., 2003, MNRAS, 345, 447
- D'Odorico, V., Petitjean, P., 2001, A&A, 370, 729
- Ferland, G. J., 2005, <http://www.nublado.org>
- Haardt, F., Madau, P., 2001, <http://pitto.mib.infn.it/~haardt/refmodel.html>
- Prochaska, J. X., Gawiser, E., Wolfe, A. M., Castro, S., Djorgovski, S. G., 2003, ApJ, 595, L9
- Schaye, J., 2001, ApJ, 559, 507
- Schaye, J., Aguirre, A., Kim, T.-S., Theuns, T., Rauch, M., Sargent, W. L. W., 2003, ApJ, 596, 768
- Songaila, A., Cowie, L. L., 1996, ApJ, 112, 335